Available online at www.sciencedirect.com
SCIENCE DIRECT®
Chemical Physics Letters 377 (2003) 399–405
CHEMICAL PHYSICS LETTERS
www.elsevier.com/locate/cplett

First-principle path integral study of DNA under hydrodynamic flows

Shilong Yang, James B. Witkoskie, Jianshu Cao *

Department of Chemistry, Massachusetts Institute of Technology, Cambridge, MA 02139, USA

Received 9 April 2003; in final form 1 July 2003
Published online: 30 July 2003

Abstract

We use the worm-like chain as a first-principles model to study single molecule experiments of double stranded DNA subject to constant plug, elongational, and shear flows. The steady-state configurations of the polymer correspond to a locally defined potential and result in a path integral description of the canonical partition function. The parameters of this model are consistent with previous theory and experimental measurements. The time averaged mean extension reproduces experimental results and compares well with computationally more expensive Brownian dynamics simulations of reduced models.

1. Introduction

The mechanical properties of polymer systems are important in many applications, including lubricants and plastics. The bulk visco-elastic properties of these systems result from the microscopic deformation of the polymer chains when they are subject to external forces. This microscopic–macroscopic correspondence has generated interest in studying polymeric solutions at the microscopic level, including experiments at the single molecule level. Many single molecule experiments examine the behavior of single polymers, like DNA, subject to various stresses, including tensile stress and hydrodynamic flow [1–11]. One set of experiments by Chu's group monitor fluorescently labeled DNA subject to the stresses discussed above. The experiment monitors the entire contour in real time and gives a complete picture of the polymer dynamics [5–15]. In this Letter, we model DNA as a worm-like chain (WLC) with parameters previously determined in force–extension experiments and then use this model to examine the experimental results of Chu for the steady-state configurations of DNA subject to constant plug, elongational, and shear flows [4–11]. The ability to use parameters from one experiment to model different experiments confirms the validity of the WLC model for DNA.

This DNA system has also been the subject of many Brownian dynamics simulations [16–21]. Predicting the properties of a complete contour,

* Corresponding author. Fax: +1-617-253-7030.
E-mail address: jianshu@mit.edu (J. Cao).

0009-2614/$ - see front matter © 2003 Elsevier B.V. All rights reserved.
doi:10.1016/S0009-2614(03)01135-7

requires a large number of long simulations performed on a large number of beads. With carefully chosen parameters, reasonable agreement between the experiments and these simulations exists, but these calculations are phenomenological and computationally intensive [17]. We propose a less computationally intensive first-principles path integral Monte Carlo algorithm based on equilibrium theory to study DNA subject to various hydrodynamic flows. If the relaxation of the polymer is fast, the experimentally observed configurations correspond to a generalized equilibrium distribution, which has an associated potential. With a reasonable formulation of the potential, we evaluate time averaged ensemble quantities with Monte Carlo techniques. Although this approach will not describe dynamics, it is computationally more efficient than Brownian dynamics and allows the prediction of important time averaged quantities, like the mean extension of the polymer that we examine in this Letter. Previously, Larson et al. [22] used similar Monte Carlo techniques on bead and spring models to describe time averaged properties of DNA polymers subject to constant plug flow.

DNA is a difficult polymer to model because it is semi-flexible with a large persistence length of 53 nm, compared to a typical length studied in experiments of 50 μm, and its contour length only extends under strong forces [17,22]. Bead and spring simulations require a large number of beads to account for bending energy and constrained dynamics to maintain the contour length. We adopt a more natural model for DNA, the WLC model of Kratky and Porod [23]. The WLC replaces the Rouse-like bead and spring model with a continuous contour of fixed length and includes an energy associated with bending the polymer. The bending energy is experimentally measurable, which removes a fitting parameter. The first analytic treatment of the WLC model appears in a 1973 paper by Fixman and Kovac [24]. Later work by Marko and Siggia with improvements by Bouchiat demonstrate that the WLC model predictions agree extremely well with the force–extension experiments on DNA by Bustamante's group [25]. The agreement suggests that the WLC captures the fundamental thermodynamics of DNA [1,9,26]. The WLC is also the basis for the force–extension relations used in simulations by Doyle and in the analytic theory by Zimm [17,27]. Doyle neglects hydrodynamic interactions while Zimm incorporates the interactions with a length dependent rescaling of the flow field determined by the Kirkwood approximation.

In the absence of an external field, the energy of the WLC is a simple contour integral, $\beta E = \int_0^L A/2|\partial_s \hat{\mathbf{t}}|^2 \, \mathrm{d}s$, where L is the polymer's length [24]. The inverse temperature, β makes all quantities unitless and the tangent vector $\hat{\mathbf{t}}$ of the contour $\mathbf{R}(s)$ is normalized to fix the contour length, $|\hat{\mathbf{t}}| = 1$. An external potential, $\beta U(\mathbf{R}(s))$ modifies the energy resulting in a path integral partition function,

$$Z = \int D\mathbf{R}(s) \times \exp\left(- \int_0^L \left\{ \frac{A}{2} |\partial_s \hat{\mathbf{t}}|^2 + \beta U(\mathbf{R}(s)) \right\} \mathrm{d}s \right). \quad (1)$$

We can derive the form of $\beta U(\mathbf{R}(s))$ for many experiments. For example, in the experiments of Smith et al. [9], one end of the DNA strand is attached to a glass surface and magnetic tweezers stretch the other end of the DNA. The external potential is

$$U(\mathbf{R}(s)) = -f|R_z(0) - R_z(L)| = -f \left| \int_0^L \hat{t}_z \, \mathrm{d}s \right|,$$

where f is the force applied to the two ends and $\hat{t}_z$ is the component of the tangent vector in the direction of the force. The solution maps into the trajectory of a quantum rigid-rotor and has good agreement with experiment [1,24,26]. We parameterize the bending energy of the WLC model with the persistence length determined by these references, $A = 53$ nm, to remove fitting parameters and validate the consistency of the WLC description of DNA in various experiments. We neglect the persistence length's dependence on various experimental conditions, such as buffer concentrations and the dye used in imaging.

The potential is not easily defined for hydrodynamic flows because hydrodynamic flows are dynamic phenomenon, but the flow still performs

work on each monomer. If we ignore the intra-chain hydrodynamic interactions of a polymer in a potential flow, like constant plug flow or elongational flow, the work is proportional to differences in the potential. For a free-draining polymer, we add the potential of all of the monomer units, which becomes an integral over the contour. A simple double integral over the contour can incorporate the two body potential, but this is not done here. Removal of the free draining approximation is more difficult, but previous studies show that hydrodynamic interactions lead to only modest corrections to many time averaged quantities [21,22].

2. Constant plug flow

The constant plug flow potential is $V = -F \cdot z$, where F is the flow rate, and the polymer's potential is $-F\xi \int_0^L z(s)\,\mathrm{d}s$, where ξ is the friction per unit length. Based on the findings of Larson et al. [22], we assume the friction does not vary with the flow rate or over the polymer, but we do not know the friction constant explicitly. Most experiments report the viscosity of the polymer in the solution, whose relation to friction has a non-trivial geometric dependence. The friction is the only fitting parameter, but it is comparable in all simulations and simply scales the flow rates. The Kirkwood approximation in Zimm's calculation for constant plug flow replaces the bare uniform force on each segment from the flow field with a dressed force that is also uniform and justifies a rescaled friction constant [27].

Perkins et al. [6] performed the constant flow experiment with optical tweezers. Fluid passes over the polymer creating a force along the entire polymer. Integration by parts gives an insightful formula for the potential, $-F \cdot \xi \int_0^L (L-s)\hat{t}_z\,\mathrm{d}s$. The energy of the potential comes from a tension that scales linearly along the chain. The tension is the greatest at the end tethered to the bead because the whole chain pulls on this end, and it lessens further down the chain until it becomes zero at the free end. For a strong flow, the polymer is almost completely extended in the z-direction, and the components in the x and y directions are small perturbations of the linear configuration. The energy of the WLC is approximately

$$\beta E \approx \int_0^L \left[A/2|\partial_s \hat{\mathbf{t}}_\perp|^2 + F\xi(L-s)|\hat{\mathbf{t}}_\perp|^2\right] - \frac{F}{2}L^2, \tag{2}$$

where $\hat{\mathbf{t}}_\perp$ is the transverse components of the tangent vector, the x and y directions, and the component in the z-direction is approximately $t_z = 1 - (1/2)|\hat{\mathbf{t}}_\perp|^2$ [26]. The action corresponds to a quantum harmonic oscillator with a linearly ramped spring constant. The x and y components act independently and the partition function for each component is Gaussian

$$\begin{aligned}\int \mathscr{D}(\hat{\boldsymbol{t}}_\perp^{(x,y)}(s)) \exp\Bigg(&-\frac{A}{2}\hat{\boldsymbol{t}}_\perp^{(x,y)}(s)\frac{\mathrm{d}\hat{\boldsymbol{t}}_\perp^{(x,y)}(s)}{\mathrm{d}s}\Bigg|_0^L \\ &+ \int_0^L\int_0^L \mathrm{d}s\,\mathrm{d}s'\delta(s-s')\Bigg\{\frac{A}{2}\hat{\boldsymbol{t}}_\perp^{(x,y)}(s')\frac{\mathrm{d}^2\hat{\boldsymbol{t}}_\perp^{(x,y)}(s)}{\mathrm{d}s^2} \\ &- \hat{\boldsymbol{t}}_\perp^{(x,y)}(s')\frac{F\xi}{2}(L-s)\hat{\boldsymbol{t}}_\perp^{(x,y)}(s)\Bigg\}\Bigg).\end{aligned} \tag{3}$$

Since the operator in the exponential is Hermitian, the Green's function for the average square of the transverse component, $u(s,s') = \langle(\hat{\boldsymbol{t}}_\perp^{(x,y)})(s)(\hat{\boldsymbol{t}}_\perp^{(x,y)})(s')\rangle$, is a weighted sum of eigenfunctions, $G(s,s') = \sum_n |u_n(s)\rangle\lambda_n^{-1}\langle u_n(s')|$, that satisfy the differential equation

$$-A\frac{\mathrm{d}^2 u_n(s)}{\mathrm{d}s^2} + F\xi(L-s)u_n(s) = \lambda_n u_n(s), \tag{4}$$

with the boundary conditions $u_n'(0) = u_n'(L) = 0$. The analytic solutions to the equation are sums of Bessel functions. The rms of the traverse displacement is $\sqrt{\sum_n \lambda_n^{-1}|\int_0^L u_n(s)\,\mathrm{d}s|^2}$, which is shown in Fig. 1. Since $\langle t_z\rangle \approx 1 - (1/2)(\langle(\hat{\boldsymbol{t}}_\perp^{(x)}(s))^2\rangle + \langle(\hat{\boldsymbol{t}}_\perp^{(y)}(s))^2\rangle) = 1 - \sum \lambda_n^{-1}u_n^2(s)$, the average extension in the z-direction is approximately $L - \sum \lambda_n^{-1}\int_0^L \mathrm{d}s\,u_n^2(s) = L - \sum \lambda_n^{-1}$. Since the eigenvalues change slowly with the flow rate in the high stretching regime, the width and extension also change slowly. The rms displacement displays a trumpet shape that is qualitatively similar to the shapes observed in experiments, simulations, and other theories [6,22,28,29].

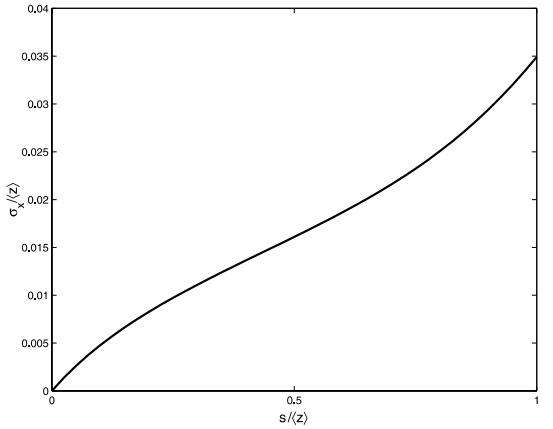

Fig. 1. The root mean square displacement of the traverse component of the polymer in a strong constant plug flow. The displacement is plotted as a function of distance in the direction of the flow field. Note the resemblance to the trumpet shape observed in experiment and simulation.

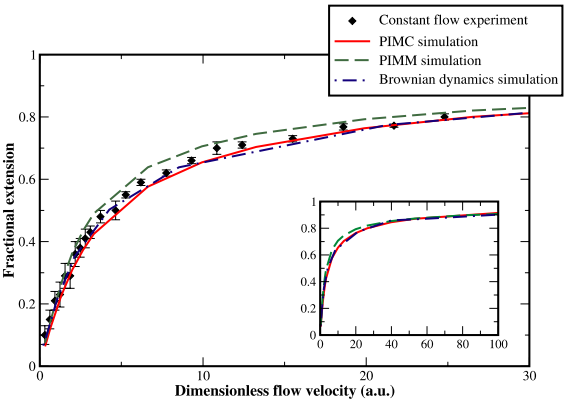

Fig. 2. Comparison of the constant plug flow experiment in [6], the path-integral Monte Carlo simulation, the path-integral matrix multiplication method, and the Brownian dynamics simulation reported in [17]. Inset compares asymptotic behavior of the simulations for large flow rates.

Without the the large flow rate approximation, the action of the tangent vector corresponds to the imaginary time Schrödinger equation for a rigid-rotor in a time dependent potential

$$\frac{\partial \Psi(s)}{\partial s} = \left[\frac{\hat{\mathbf{L}}^2}{2A} + F\xi(L-s)\cos(\theta)\right]\Psi(s). \tag{5}$$

In this equation, $\hat{\mathbf{L}}$ is the angular momentum operator, and $\cos(\theta)$ is the projection of the tangent vector onto the direction of the flow field. This equation resembles the constant force calculations with a simple time dependence $(L-s)$ [26]. This equation can be solved by using a spherical harmonic basis set and numerically propagating the resulting matrix [1,26]. The only difficulty is the initial condition of the wavefunction, for which we use results that are consistent with the high stretching calculation above, $t_z(0) = 1$ and $t_z(0) = t_y(0) = 0$.

Fig. 2 compares the predictions of mean fractional extension versus flow rate for the rotor Hamiltonian, the Monte Carlo simulation discussed below, the experimental results of Perkins et al. [6,17], and the Brownian dynamic simulations of Doyle. Since the experiment cannot determine the end-to-end distance, the fractional extension is the maximum distance between any points on the polymer contour compared against the contour length. The flow rate is in a dimensionless form, $Wi = \tau_F/\tau_p$, where τ_F is the characteristic time of the flow and τ_p is the longest relaxation rate of the free polymer, which is determined by equations in [17–19]. For elongational and shear flows, the dimensionless form corresponds to Weissenberg numbers. Both simulations compare well with experiment. The mean extension initially increases rapidly with the flow rate. At about 60% of full extension, the rate of increase in the extension slows to an asymptotic approach to full extension in the large flow rate limit.

A slight discrepancy for moderate flow rates results from the initial condition, which is correct in the strong stretching limit and is not important for weak flows. Monte Carlo techniques correct the discrepancy, as would different initial conditions, which are not done here to avoid additional fitting parameters. Although we do not present these results since they appear elsewhere, the matrix multiplication method exactly reproduces the constant force results of Bouchiat, which agrees with the experiments of Bustamante, since no ambiguity about the initial conditions exists, and the rigid-rotor equation is the same [1,9,25,26].

3. Elongational flow

The quantum rigid-rotor analogy extends to the elongational flow by changing the form of the external potential to

$$-F\xi \int_0^L \mathrm{d}s(z^2(s) - 1/2(x^2(s) + y^2(s))),$$

where F is the flow rate over length. The potential depends on the position instead of the tangent vector. Unless we know the starting position, which depends on the steady-state distribution, we do not know $\mathbf{R}(s)$ and cannot predict the s dependence of the field. To overcome the difficulties presented by this potential, we evaluate the path integral using Monte Carlo techniques.

As a calibration, we analyze the constant plug flow experiment with Monte Carlo and compare these results with our previous results. We discretized the polymer into 844 segments, two segments per persistence length for a DNA chain that is 22.4 μm in length. The discretization captures the rigidity of the polymer without incorporating phenomenological bending springs. The segments are fixed in length and only the angles are varied. We fix one end of the polymer at the origin and perform 12×10^6 Monte Carlo steps with the potential energy defined above. The Monte Carlo algorithm fits the experiment and Brownian dynamic simulation results better than the matrix multiplication method, as shown in Fig. 2. These results give us confidence in using this algorithm to evaluate more complicated flows.

Elongational flow corresponds to the experiments of Smith and Chu and of Perkins et al. [7,10]. In these experiments, the DNA is freely flowing with the fluid. Since the forces caused by this flow are linear, we decompose the motion of the polymer into center of mass and relative motion of the polymer segments. The Monte Carlo procedure is the same as for the constant plug flow, except that the energy is determined in the relative coordinate frame. Fig. 3 shows the fractional extension results compared against the experimental results of Chu and the Brownian dynamic simulations of Doyle [17].

Even for this more complicated flow, the fractional extensions predicted by both of the simulations agree extremely well with the experimental results. The fractional extension as a function of flow rate rises quickly to about 80% before a slow asymptotic approach to full extension. In the strong flow limit, the Monte Carlo simulation slightly overestimates the extension, as compared to the experiment and Brownian dynamics simulation, but all three results agree extremely well for weak and moderate flows. The agreement between the simulations and experiments for the constant plug and elongational flows demonstrates that the Monte Carlo technique successfully reproduces the results for potential flows and that the WLC model is a good description of DNA and possibly other semi-flexible biological polymers in potential flows.

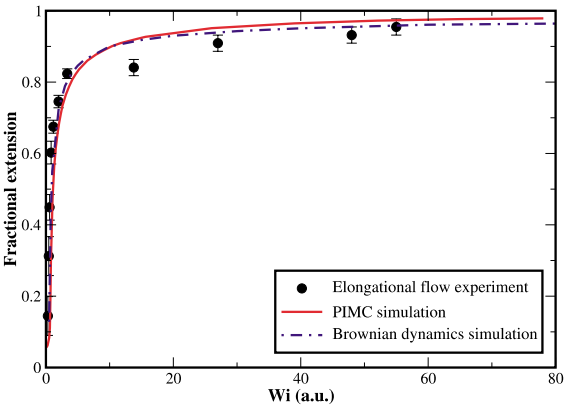

Fig. 3. Comparison of the elongational flow experiment in [7], the path-integral Monte Carlo simulation, and the Brownian dynamics simulation reported in [17].

4. Shear flow

Encouraged by the success of the path integral Monte Carlo method on potential flows, we investigate the application of these methods to non-conservative flow fields like shear flow. The simple shear flow also has an analogous rigid-rotor Hamiltonian with an electrostatic potential $U \propto -x \cdot z$ and a non-conservative B-field, $\hat{\mathbf{r}} \times \hat{\mathbf{y}}$, where $\hat{\mathbf{r}}$ is the position vector and $\hat{\mathbf{y}}$ is the unit vector in the y-direction. Similar to the elongational flow, we avoid the difficulty of the position

dependence by evaluating the action with Monte Carlo.

The shear flow experiment that we analyze is similar to the elongational flow experiment [11,17]. The DNA freely flows with the fluid, and we calculate the forces in the center of mass frame using the simple shear relations, $F_z = F\xi x$ and $F_x = F_y = 0$, where F is flow rate over length. Although shear flow is not a potential flow, the fluid still performs work on the system, which allows us to define a local energy change by integrating the force along the linear path connecting two configurations. The probability of a transition occurring is proportional to the energy difference in the local frame. Several authors used this approach to describe other polymer systems in shear flows [30–33]. Since the potential changes as the polymer moves, detailed balance does not hold and the polymer rotates through space, but this simulation can be viewed as a Glauber dynamics [34]. The Monte Carlo algorithm for the shear flow follows the same steps as the constant plug flow and elongational flow with the potential defined locally. A trajectory dependence exists, which may require a larger number of simulation steps than the potential flows, but we still only use 12×10^6 Monte Carlo steps.

The force–extension relations for shear flow are plotted in Fig. 4. As with the potential flows, the path integral Monte Carlo method agrees extremely well with both experiment and the Brownian dynamics simulation. Because we only used 12×10^6 Monte Carlo steps, some scatter in the data exists. We added a trend line in Fig. 4 to help the eye follow the data. For weak shear rates there is a fast initial rise in the mean extension. After the initial rise, the data quickly asymptotes to about 40% extension. The small asymptotic value can be understood by examining the decomposition of the shear flow field into an elongational part and a rotational part. At an angle of about $\pi/4$ in the xz plane, the polymer gets stretched, but at $-\pi/4$ the polymer gets compressed [11,17,35]. The rotational part moves the polymer between these angles resulting in an averaging over these angles and a decreased total extension. This cycling from the extended to the compressed states has been observed in the experiment, the Brownian dynamics simulations, and our Monte Carlo simulations. The correspondence shows that the Glauber dynamics of a Monte Carlo simulation does capture some of the real dynamics of the system.

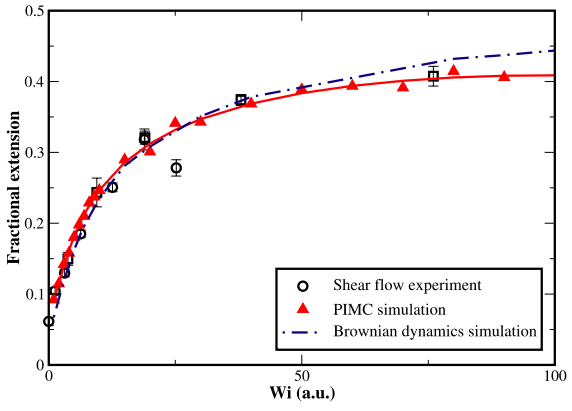

Fig. 4. Comparison of the shear flow experiment in [11], the path-integral Monte Carlo simulation, and the Brownian dynamics simulation reported in [17]. To aid the eye, the solid curve follows the trend of the Monte Carlo data.

5. Summary and conclusion

As demonstrated in this Letter, the WLC is a good model for DNA and possibly other semiflexible biopolymers. With a single fitting parameter, the friction constant, which linearly scales the flow rate, the solution to the path integral quantitatively agrees with experimental results for DNA subject to constant plug, elongational, and shear flows. The model is based on physical principles without phenomenological force–extension relations. Although hydrodynamics are strictly dynamic phenomenon, time averaged quantities are quasi-equilibrium phenomenon in an effective potential. This description is possible because relaxation to the steady-state distribution is fast and contributions from intra-chain hydrodynamics can often be neglected. The equilibrium partition function corresponds to an ensemble average, which demonstrates the correspondence between time-averages of single molecule trajectories and ensemble averages for ergodic systems. These

techniques are computationally inexpensive since we do not have to run many trajectories to average over initial distributions. This path integral approach is applicable to other semi-flexible biopolymer systems.

Acknowledgements

We thank S. Chu, D.E. Smith, T.T. Perkins, and P. Doyle for sharing their data. This research is supported by the AT & T Research Fund Award and the NSF Career Award (No. Che-0093210).

References

[1] C. Bouchiat, M.D. Wang, J.F. Allemand, T. Strick, S.M. Block, V. Croquette, Biophys. J. 76 (1999) 409.
[2] T.R. Strick, J.F. Allemand, D. Bensimon, A. Bensimon, V. Croquette, Science 271 (1996) 1835.
[3] P. Cluzel, A. Lebrun, C. Heller, R. Lavery, J.L. Viovy, D. Chatenay, F. Caron, Science 271 (1996) 792.
[4] H.P. Babcock, D.E. Smith, J.S. Hur, E.S.G. Shaqfeh, S. Chu, Phys. Rev. Lett. 85 (2000) 2018.
[5] T.T. Perkins, S.R. Quake, D.E. Smith, S. Chu, Science 258 (1992) 1122.
[6] T.T. Perkins, D.E. Smith, R.G. Larson, S. Chu, Science 268 (1995) 83.
[7] T.T. Perkins, D.E. Smith, S. Chu, Science 276 (1997) 2016.
[8] S.R. Quake, H. Babcock, S. Chu, Nature 388 (1997) 151.
[9] S.B. Smith, L. Finzi, C. Bustamante, Science 258 (1992) 1122.
[10] D.E. Smith, S. Chu, Science 281 (1998) 1335.
[11] D.E. Smith, H.P. Babcock, S. Chu, Science 283 (1999) 1724.
[12] P. Thomen, U. Bockelmann, F. Heslot, Phys. Rev. Lett. 88 (2002) 8102.
[13] R.W. Hammond, X.L. Shi, M.D. Morris, J. Microcolumn Sep. 44 (2000) 713.
[14] X.L. Shi, R.W. Hammond, M.D. Morris, Polymer 42 (2001) 8483.
[15] I. Auzanneau, C. Barreau, L. Salome, Comptes Rendus De L Academi Des Sciences Serie III- Sciences De La Vie-Life Sciences 316 (1993) 459.
[16] N.C. Andrews, A.J. McHugh, J. Reol. 42 (1998) 281.
[17] P.S. Doyle, B. Ladoux, J.L. Viovy, Phys. Rev. Lett. 84 (2000) 4769.
[18] P.S. Doyle, E.S.G. Shaqfeh, G.H. McKinley, S.H. Spiegelberg, J. Non-Newtonian Fluid Mech. 76 (1998) 79.
[19] P.S. Doyle, E.S.G. Shaqfeh, A.P. Gast, J. Fluid Mech. 334 (1997) 251.
[20] J.S. Hur, E.S.G. Shaqfeh, R.G. Larson, J. Rheol. 44 (2000) 713.
[21] R.M. Jendrejack, J.J. de Pablo, M.D. Graham, J. Chem. Phys. 116 (2002) 7752.
[22] R.G. Larson, T.T. Perkins, D.E. Smith, S. Chu, Phys. Rev. E 55 (1997) 1794.
[23] M. Doi, S.F. Edwards, Theory of Polymer Dynamics, Cambridge University Press, Cambridge, 1986.
[24] M. Fixman, J. Kovac, J. Chem. Phys. 58 (1973) 1565.
[25] C. Bustamante, J.F. Marko, E.D. Siggia, S. Smith, Science 265 (1994) 1599.
[26] J.F. Marko, E.D. Siggia, Macromolecules 28 (1995) 8759.
[27] B.H. Zimm, Macromolecules 31 (1998) 6089.
[28] P.G. De Gennes, J. Chem. Phys. 60 (1974) 5030.
[29] F. Brochard-Wyart, Europhys. Lett. 30 (1995) 387.
[30] Y.P. Lai, K. Binder, J. Chem. Phys. 98 (1993) 2366.
[31] S. Tan, Polymer 40 (1999) 695.
[32] L. Miao, H. Guo, M.J. Zuckermann, Macromolecules 29 (1996) 2289.
[33] G. Xu, J. Ding, Y. Yang, Rheol. Acta 40 (2001) 60.
[34] J.M. Nunes Da Silva, E.J.S. Jage, Phys. Lett. A 135 (1989) 17.
[35] B. Ladoux, P.S. Doyle, Europhys. Lett. 52 (2000) 511.